Assembly of Fullerene Arrays Templated by DNA Scaffolds

Cheng Song,[†,‡] Ya-Qing Chen,[†] Shou-Jun Xiao,*[,†] Long Ba,[§] Zhong-Ze Gu,[§] Yi Pan,[†] and Xiao-Zeng You[†]

State Key Laboratory of Coordination Chemistry, School of Chemistry and Chemical Engineering, Nanjing University, 22 Hankou Road, Nanjing 210093, People's Republic of China, School of Chemistry and Chemical Engineering, Jiangxi Normal University, Nanchang 330046, People's Republic of China, and State Key Laboratory of Molecular and Biomolecular Electronics, Southeast University, Nanjing 210096, People's Republic of China

Received July 21, 2005
Revised Manuscript Received November 3, 2005

Much effort has been devoted to the assembly of nanoparticles into arrays because the array is of interest both for foundamental and practical research. For example, arrays of nanoparticles can be applied in molecular electronic junctions, light-emitting diodes, single electron transistors, nanooptics, and nano-electronic circuits. A particular approach is the fabrication of arrays by means of biomolecular templates. Loweth et al.[1] reported the preparation of stoichimetric conjugates of gold nanoparticles with mercaptolized oligonucleotides and then the assembly of nanoparticles into dimmers and trimers guided by the hybridization of these conjugates to the linear double helix. Mirkin et al.[2] observed the color change between red and purple because of the reversibility of nanoparticle aggregates by cycling the oligo hybridization temperature. Niemeyer and co-workers[3] used a hybrid DNA−protein strategy (DNA−streptavidin conjugates) to assemble Au nanoparticles along a long DNA template. Ongaro et al.[4] used DNA as a template to assemble protein−gold conjugates for fabrication of nanogap electrodes. Novak et al.[5] assembled the nanoparticle arrays with a rigid organic molecule−phenylethynyl thiols. A fascinating template−DNA lattice,[6] developed by Seeman's group, is attracting more attention for assembly of 2D arrays of nanoparticles and proteins. Kiel and co-workers[7,8] reported the Au nanoparticle arrays, assembled by introducing the conjugate of gold−oligo as a component into the 2D DNA scaffolding either during its growth or by post-hybridization after the formation of DNA lattices. Reif and co-workers[9,10] reported the protein arrays, built up by incorporating biotin-labeled thymidines into the 2D DNA lattice with modulated patterns and then the attachment of streptavidin. Our strategy is shown in Figure 1.

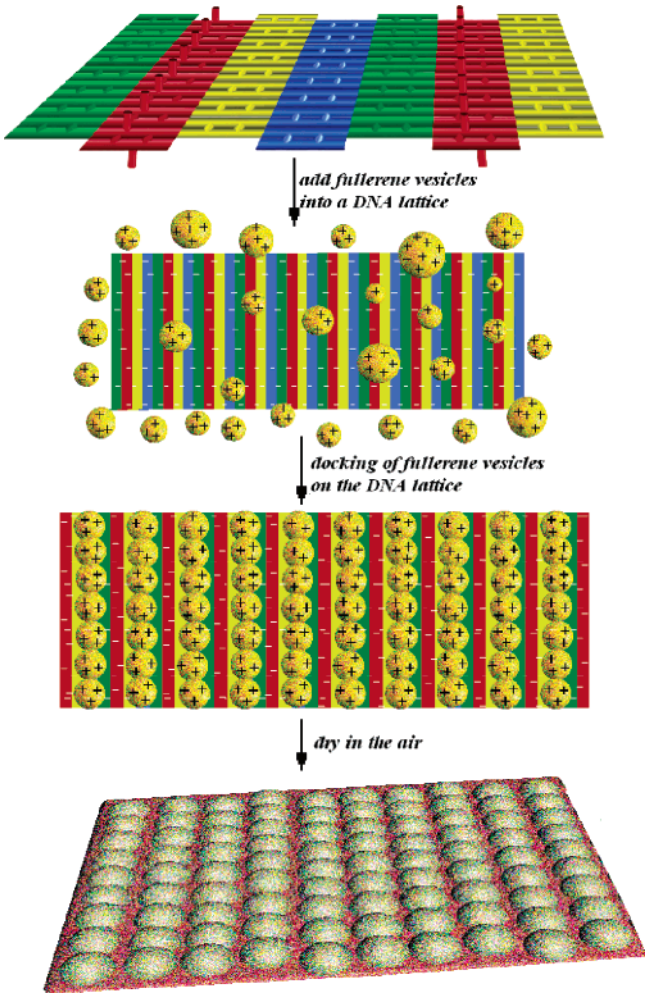

Figure 1. Sketch of the self-assembly procedure of fullerene vesicles on the 2D DNA scaffolding. First, a DNA scaffolding is assembled in an aqueous buffer according to the work of Seeman's group.[11] Four tiles are represented by yellow (A), red (B), green (C), and blue (D). Tile B (red) bears two protruding structures (2J), one to the upper side and the other to the backside of the DNA scaffolding plane. The upper J carries an end group of phosphate. Second, a suspension of fullerene vesicles is added. Third, fullerene vesicles are docked to the scaffolding and arranged as arrays. Finally, the vesicles collapse to form four-layered domains after drying.

In our experiments, similar sequences of DNA codes to Seeman's work[11] are employed to fabricate 2D DNA crystals. These sequences contain a set of 22 designed synthetic oligonucleotides in Figure S1 of Supporting Materials, which can assemble into four DX tiles A, B, C, and D, respectively.

* Corresponding author e-mail: sjxiao@nju.edu.cn.
† Nanjing University.
‡ Jiangxi Normal University.
§ Southeast University.

(1) Loweth, C. J.; Caldwell, W. B.; Peng, X.; Alivisatos, A. P.; Schultz, P. G. *Angew. Chem., Int. Ed.* **1999**, *38* (12), 1808−1812.
(2) Mirkin, C. A.; Letsinger, R. L.; Mucic, R. C.; Storhoff, J. J. *Nature* **1996**, *382*, 607−609.
(3) (a) Zou, B.; Ceyhan, B.; Simon, U.; Niemeyer, C. M. *Advanced Materials*, early view. (b) Niemeyer, C. M.; Burger, W.; Peplies, J. *Angew. Chem., Int. Ed. Engl.* **1998**, *37*, 2265−2268.
(4) Ongaro, A.; Griffin, F.; Nagle, L.; Iacopino, D.; Eritja, R.; Fitzmaurice, D. *Adv. Mater.* **2004**, *16* (20), 1799−1803.
(5) Novak, J. P.; Nickerson, C.; Franzen, S.; Feldheim, D. L. *Anal. Chem.* **2001**, *73*, 5758−5761.
(6) Winfree, E.; Liu, F.; Wenzler, L. A.; Seeman, N. C. *Nature* **1998**, *394*, 539−544.
(7) Xiao, S. J.; Liu, F.; Rosen, A.; Hainfeld, J. F.; Seeman, N. C.; Musier-Forsyth, K.; Kiehl, R. A. *J. Nanopart. Res.* **2002**, *4*, 313−317.
(8) Le, J. D.; Pinto, Y.; Seeman, N. C.; Kiehl, R. A. *Nano. Lett.* **2004**, *4*, 2343−2347.
(9) Yan, H.; Park, S. H.; Finkelstein, G.; Reif, J. H.; LaBean, T. H. *Science* **2003**, *301*, 1882.
(10) Park, S. H.; Yin, P.; Liu, Y.; Reif, J. H.; LaBean, T. H.; Yan, H. *Nano Lett.* **2005**, *5*, 729−733.
(11) Liu, F.; Sha, R.; Seeman, N. C. *J. Am. Chem. Soc.* **1999**, *121*, 917−922.

10.1021/cm051606v CCC: $30.25
Published on Web 12/03/2005

The four tiles are the building blocks for construction of DNA lattices. The crystals are grown in an aqueous buffer by slowly decreasing the temperature from 95 °C to 4 °C within 48 h. Two protruding structures (2J) in tile B are designed as (i) markers for imaging and (ii) accessories for introduction of functional molecules. They form the featured structure of parallel stripes in TEM and AFM images, where the distance between the nearest neighboring stripes is 64 nm.

Water-soluble fullerenes have been reported to form vesicles in an aqueous solution or in a mixture of water/organic solvent within a short time less than 1 h. Careful laser light scattering studies in Chu's laboratory[12] showed that spherical bilayer aggregates of 34 nm average diameter were formed upon slow injection of a THF solution to water. Similar to the lipid vesicles, the fullerene vesicles are somehow flexible and mobile in solution, and their membrane possesses a double layer of fullerene molecules where the hydrophilic amino groups are exposed to water with positive charges. Once they are deposited on solid surfaces, their skeleton is not robust enough to keep the ball shells. They collapse into four-layered fullerene domains. As a result, our AFM images on dried mica only exhibited the domains of collapsed vesicles. Obviously after collapse, the round domains on the supporting surface will have a diameter two times the original diameter of vesicles in the solution, forming completely extended and/or stacked multilayers. Cassell et al.[13] has reported that the fullerene domains exhibited a diameter ranging from 10 to 70 nm and a thickness from 3 to 6 nm by TEM. These results correspond very well to the laser scattering experiments. Other reports[14] indicated vesicles with diameters of 20−100 nm, which are dependent on the fullerene species, solvents, and the preparation procedure. C_{60}-*N*,*N*-Dimethylpyrrolidinium iodide (**1**)

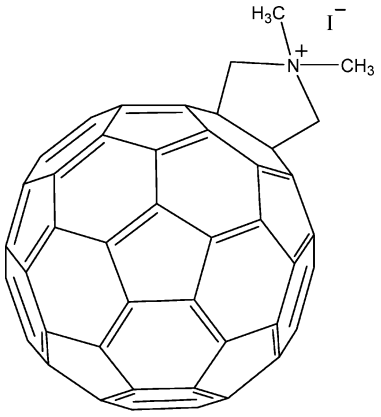

1

(0.368 mg), synthesized according to refs 15 and 16, was first dissolved in 50 μL of DMSO, then diluted to 1 mL by adding 950 μL of distilled water, and finally immersed in an ultrasonic bath for 12 h to form vesicles. The insoluble suspended species was removed through centrifugation. The resulted homogeneous solution was then used for AFM imaging and for fullerene/DNA interaction. A drop of the fullerene solution was transferred onto a mica surface, and the droplet was hung upside-down in air for a spontaneous drying. After drying, the droplet area was imaged with AFM. A representative image in Figure 2 reveals clearly the round domains. These domains exhibit the collapsed fullerene vesicles. They have diameters ranging from 20 to 100 nm, where the species within diameters less than 60 nm occupies 70%. It indicates that the vesicles with diameters of less than 30 nm dominate the fullerene solution. The average height of domains is measured as 2.5 ± 0.5 nm. Since the diameter of a fullerene molecule is 0.9 nm, the theoretical thickness of the closely packed four layer is 2.8 nm (hcp) or 3.1 nm (fcc). The calculated and measured values are very much in accordance.

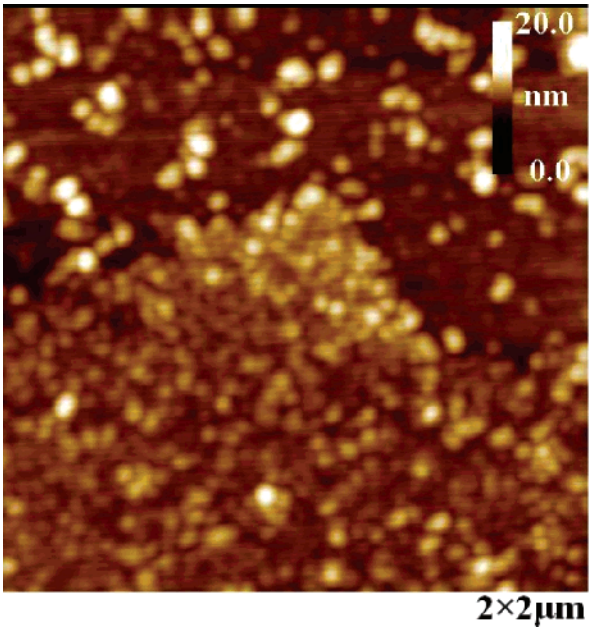

Figure 2. AFM image of collapsed fullerene vesicles.

The periodic distance 64 nm of the parallel stripes in DNA lattices are big enough for the fullerene vesicles to be docked. The prepared fullerene vesicle (0.4 mM, 0.5−10 μL) was added to 50 μL of DNA lattice (0.4 μM), respectively, and incubated overnight. Then 3−5 μL of the solution was deposited on a mica surface in a sealed saturated vapor environment, incubated for 3 min, washed with 100 μL of water 3 times, and finally air-dried for AFM imaging. Figure 3 shows the AFM topographies of the surface species. Figure 3a−c was taken under the same AFM tip in order to eliminate the different curvatures of individual tips. The plane ABCD crystal shows the same feature reported by Seeman and co-workers.[7,8] The crystal region can be divided into two featured areas: the higher stripe area and the lower wide-plateau area. However, in the fullerene-assembled DNA crystals, the image shows the reverse direction: the lower

(12) Zhou, S. Q.; Burger, C.; Chu, B.; et al. *Science* **200**1, *291* (5510), 1944−1947.
(13) Cassell, A. M.; Asplund, C. L.; Tour, J. M. *Angew. Chem., Int. Ed.* **1999**, *38* (16), 2403−2405.
(14) Georgakilas, V.; Pellarini, F.; Prato, M.; Guldi, D. M.; Melle-Franco, M.; Zerbetto, F. *Proc. Natl. Acad. Sci. U.S.A.***2002**, *99* (8), 5075−5080.
(15) Maggini, M.; Scorrano, G. *J. Am. Chem. Soc.* **1993**, *115*, 9798−9799.
(16) Bullard-Dillard, B.; Creek, K. E.; Scrivens, W. A.; Tour, J. M. *Bioorg. Chem.* **1996**, *24*, 376−385.

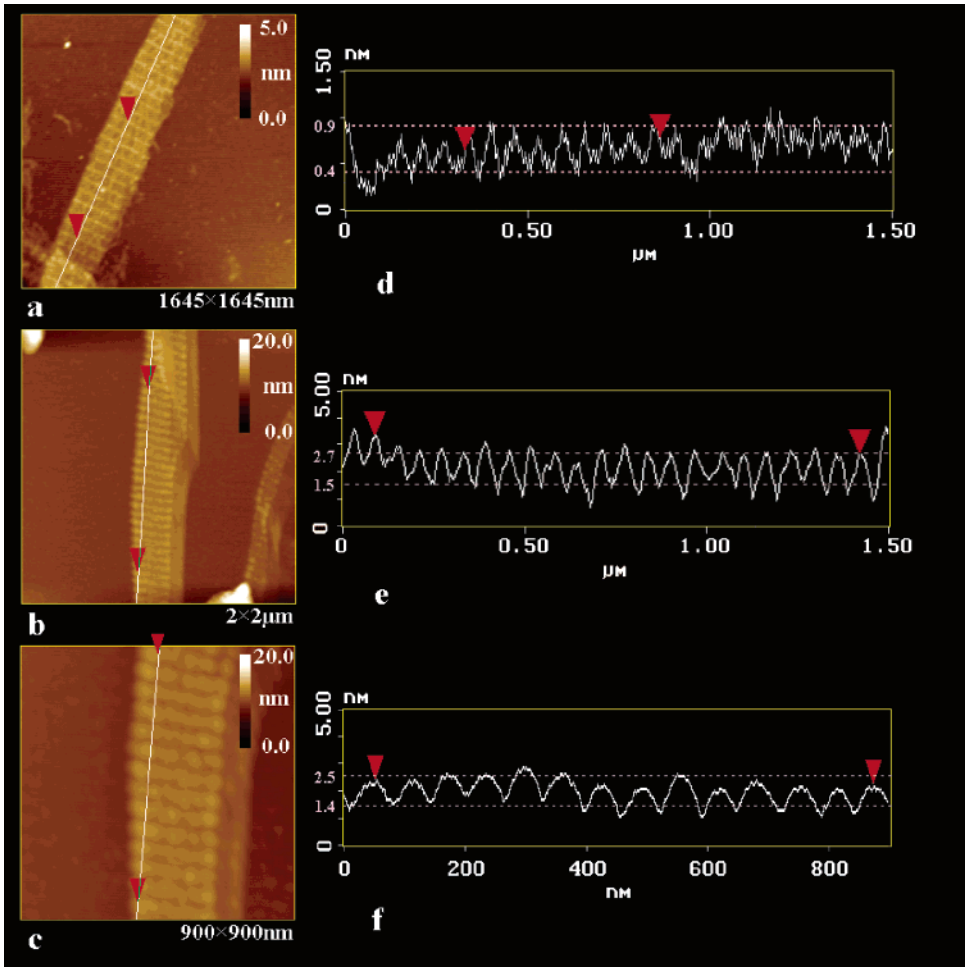

Figure 3. DNA scaffolding before and after self-assembly of the fullerene vesicles. (a) Topographical AFM images of the DNA scaffolding. Brighter (taller) diagonal ridges correspond to rows of the topographical marker—hairpins attached to tile B—and a fainter wide plateau to other DNA tiles of C, D, A, and part of B. The measured spacing between the nearest stripes is 64.0 nm. (b and c) AFM images of fullerene arrays in the DNA scaffolding. Fullerene vesicles are attached on the wide plateau region. (d) Height profile along the line shown in panel a. The height of the stripe is ~0.9, and the plateau region ~0.4 nm. (e) Height profile along the line shown in panel b. (f) Height profile along the line shown in panel c. The mean height of the top altitude of panels b and c is 2.5−2.7 nm, corresponding to the sum of the collapsed fullerene vesicle and the plateau of a bare lattice. The valley altitude is ~1.4 nm, slightly higher than the stripe height (0.9 nm) of a bare lattice.

plateau area in the bare DNA lattices arises and becomes the higher region because the fullerene vesicles fill in. The mean height of the top altitude of fullerene-filled DNA scaffolds is around 2.5−2.7 nm in Figure 3e,f. The measured height of the bare DNA lattice is around 0.4 and 0.9 nm for the plateau area and the stripe area in Figure 3, panels a and d, respectively. From Figure 2, we know that the collapsed four-layered fullerene domains are 2.5 ± 0.5 nm high. By summing the plateau of the bare crystal and the fullerene domain, the whole height will be around 2.9 nm, corresponding to our measured value of 2.5−2.7 nm very well. The valley altitude is ~1.4 nm, slightly higher than the stripe height (0.9 nm) of a bare lattice. This can be caused by some dispersed fullerene molecules filling the valley. By drawing a straight line (Figure 3a−f) perpendicular to the parallel stripes across the DNA lattice, we can analyze the occupancy percentage of the two territories by calculating the average ratio of a peak's fwhm (full width half-maximum) over a periodic distance. On the bare DNA lattice, the stripe area occupies approximately 35% of the whole lattice area; however, in the fullerene-vesicle filled lattice, the higher pear-like area occupies 70% of the whole lattice area. From the above experiments, we can conjecture that the positively charged fullerene vesicles were first aggregated into the negatively charged DNA lattices by the static Coulomb force and then modulated as pear-like arrays by the alignment of DNA scaffoldings.

Conceptually, the fullerene vesicles can be adsorbed on both planes of DNA scaffoldings. However from the height measurement, we believe that the vesicles are only adsorbed on one side of the DNA lattice. Well-ordered fullerene arrays can be observed clearly in the phosphated DNA scaffolding, and such arrays were also occasionally found in the DNA scaffolding without phosphated oligonucleotides. Therefore, phosphated oligonucleotides should play a role in the alignment of fullerene vesicles. We propose a hypothesis for the formation mechanism of fullerene arrays: The end phosphate groups in one side should bear more negative charges rather than the end neutral OH groups in the other side of the lattice. The protruding phosphated hairpins with flexible arms (12 bases and ~3.5 nm) could move freely and grab fullerene vesicles. The next step would be the docking of vesicles on the plateau area of the lattice. This process should be fast enough that the phosphate-labeled side

of the lattice could be filled up by positively charged vesicles first. After this trapping, the net charge of the whole system would become neutral, and the fullerene vesicles would not dock further on the DNA template. The protruded J structure should always squirms in the solution. This specific motion might regulate the fullerene-vesicles into parallel arrays.

We tried different assembly conditions such as concentration, pH, and incubation time. The optimum condition is as follows: a fullerene solution with about 40 times of the DNA concentration was added into the DNA lattice solution, and the solution was incubated at 4 °C and at pH 7.0−8.0 for a period of 6−12 h. Other kinds of DNA−fullerene complexes such as the big fullerene aggregates (Figure S4) were also observed occasionally. The anomalous decoration of the DNA lattice was scattered. The extreme case is the destruction of the DNA scaffolding at a high concentration of fullerene **1** over 100 times of DNA.

The main driving force for the formation of fullerene vesicles is the hydrophobicity and nondirectional intermolecular forces.[17] Different fullerene aggregates such as vesicles and rods have been reported according to their instinct nature such as the hydrophobicity and hydrophilicity of the fullerene core and the preparation conditions such as incubation time, type of sonication, presence of cosolvents, deposition, and the counterion in the buffer. It is believed that the more soluble the fullerene molecule in water, the more rod-like aggregates can be formed. In our case, the aligned fullerene arrays are directed by the presence of a templated DNA lattice. We believe that the groove effect plays a role to arrange the fullerene vesicles to form a pearl-like rod on the DNA scaffolding.

Many new physical properties have been evidenced for independent nanoparticles because of the quantization of electronic states of the structure, so for the aligned nanoparticle arrays of some novel quantum transportation effect will be expected. It is apparent that the DNA scaffolding offers the greatest advantage of programmability over other self-assembly approaches. It is the bottom-up "replica" of the top-down microelectronic technology. It can be imagined that in the future by designing the DNA building motifs one can fabricate very complicated DNA scaffolding circuits. Functional nanocomponents of molecules, nanoparticles, and biomolecules can be exactly self-assembled into the circuits by means of Watson−Crick base pairing; therefore, novel physical properties will be expected.

Acknowledgment. The authors are grateful for the financial support of the National High Technology Research and Development of Program of China (863 Program) No. 2004AA302G12 and the High Technology (Industry) Project BG2003028 of Jiangsu Province.

Supporting Information Available: Experimental section, including additional figures. This material is available free of charge via the Internet at http://pubs.acs.org.

CM051606V

(17) Israclachvili, J. N. *Intermolecular Forces*, 2nd ed.; Academic: London, 1992; pp 349−360.